Inorganic Chemistry

Article

pubs.acs.org/IC

Synthesis, Structure, and Reactivity of an Anionic Zr−Oxo Relevant to CO_2 Reduction by a Zr/Co Heterobimetallic Complex

Jeremy P. Krogman, Mark W. Bezpalko, Bruce M. Foxman, and Christine M. Thomas*

Department of Chemistry, Brandeis University, 415 South Street MS 015, Waltham, Massachusetts 02454, United States

Supporting Information

ABSTRACT: Oxidative addition of CO_2 to the reduced Zr/Co complex (THF)Zr(MesNP^{i}Pr$_2$)$_3$Co (**1**) followed by one-electron reduction leads to formation of an unusual terminal Zr−oxo anion [**2**][**Na(THF)$_3$**] in low yield. To facilitate further study of this compound, an alternative high-yielding synthetic route has been devised. First, **1** is treated with CO to form (THF)Zr(MesNP^{i}Pr$_2$)$_3$Co(CO) (**3**); then, addition of H_2O to **3** leads to the Zr−hydroxide complex (HO)Zr(MesNP^{i}Pr$_2$)$_3$Co(CO) (**4**). Deprotonation of **4** with Li(N(SiMe$_3$)$_2$) leads to the anionic Zr−oxo species [**2**][**Li(THF)$_3$**] or [**2**][**Li(12-c-4)**] in the absence or presence of 12-crown-4, respectively. The coordination sphere of the Li^+ countercation is shown to lead to interesting structural differences between these two species. The anionic oxo fragment in complex [**2**][**Li(12-c-4)**] reacts with electrophiles such as MeOTf and Me$_3$SiOTf to generate (MeO)Zr(MesNP^{i}Pr$_2$)$_3$Co(CO) (**5**) and (Me$_3$SiO)Zr(MesNP^{i}Pr$_2$)$_3$Co(CO) (**6**), respectively, and addition of acetic anhydride generates (AcO)Zr(MesNP^{i}Pr$_2$)$_3$Co(CO) (**7**). Complex [**2**][**Li(12-c-4)**] is also shown to bind CO_2 to form a monoanionic Zr−carbonate, [(12-crown-4)Li][(κ^2-CO$_3$)Zr(MesNP^{i}Pr$_2$)$_3$Co(CO)] ([**8**][**Li(12-c-4)**]). A more stable version of this compound [**8**][**K(18-c-6)**] is formed when a K^+ counteranion and 18-crown-6 are used. Binding of CO_2 to [**2**][**Li(12-c-4)**] is shown to be reversible using isotopic labeling studies. In an effort to address methods by which these CO_2-derived products could be turned over in a catalytic cycle, it is shown that the Zr−OMe bond in **5** can be cleaved using H^+ and the CO ligand can be released from Co under photolytic conditions in the presence of I_2.

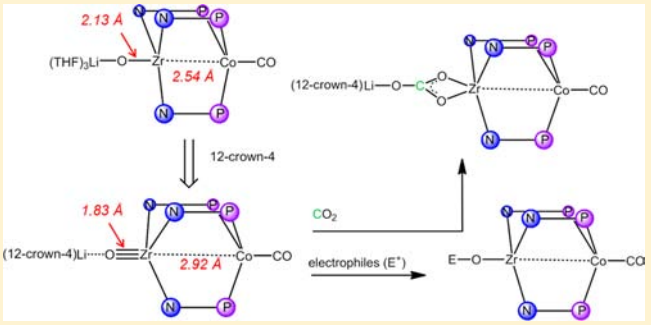

INTRODUCTION

Recent interest in the reduction of CO_2 stems from the need for a carbon-neutral alternative to fossil fuels.[1] One CO_2 activation strategy that has emerged is the use of bifunctional transition metal complexes containing a Lewis-acidic and Lewis-basic site to aid in CO_2 binding.[2−4] Early/late heterobimetallic complexes are one particular design that has sparked interest in this area;[5−7] however, one of the potential difficulties of employing an early metal in CO_2 reduction is the thermodynamic stability of the metal−oxygen bond. Often cleavage of the M−O bond relies on ligand substitution, forming another stable M−X bond (where X is a "hard" ligand). In a recent publication, we reported the oxidative addition of one of the C═O bonds of CO_2 across the metal−metal multiple bond of the reduced Zr/Co heterobimetallic complex (THF)Zr(MesNP^{i}Pr$_2$)$_3$Co (**1**) to form the oxo-bridged complex (η^2-^{i}Pr$_2$PNMes)Zr(MesNP^{i}Pr$_2$)$_2$(μ-O)Co(CO) (Scheme 1).[8] Use of an early/late heterobimetallic system such as the Zr/Co complexes shown in Scheme 1 may provide some advantages over a monometallic system for electrocatalytic reduction of CO_2. For example, the Zr/Co interaction described in our previous reports may increase the lability of a terminal Zr−oxo ligand produced from CO_2 reduction via dative donation from Co into the Zr−O σ*

Scheme 1

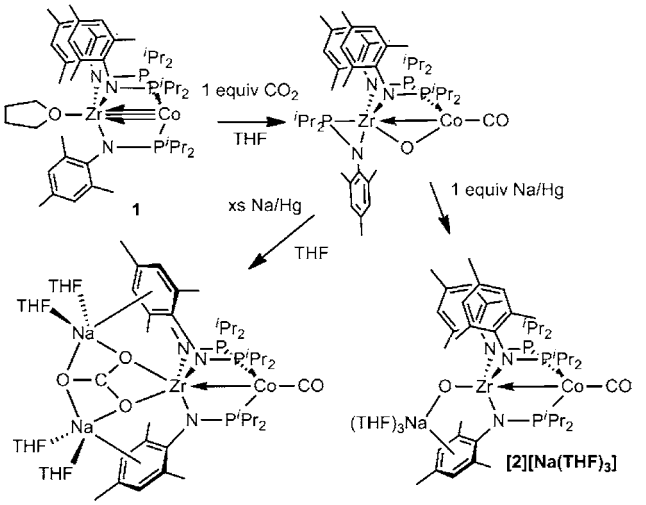

Received: November 12, 2012
Published: February 28, 2013

molecular orbital.[9−11] In addition, the dative cobalt−zirconium interaction has been shown to facilitate the two-electron reduction taking place at cobalt by shifting the reduction potentials anodically from −2.66 to −1.65 V.[10]

Upon investigating the subsequent reduction chemistry of the CO_2 activation product (η^2-^{i}Pr$_2$PNMes)Zr(MesNP^{i}Pr$_2$)$_2$(μ-O)Co(CO), we found that while the predominant product of Na/Hg amalgam reduction was the two-electron-reduced carbonate species [(THF)$_2$Na]$_2$(CO$_3$)Zr(MesNP^{i}Pr$_2$)$_3$Co(CO), careful treatment with one equivalent of reductant afforded the Zr−oxo anion [(THF)$_3$Na][OZr(MesNP^{i}Pr$_2$)$_3$Co(CO)] ([**2**][**Na(THF)$_3$**]) in low yield (Scheme 1).[8] Alternative reducing agents such as Mg^0 and Na(napthalenide) did not lead to a cleaner, more selective reaction to form [**2**]$^-$. There are few other well-defined and structurally characterized Zr−oxo anions in the literature, and the reactivity of these species has not been reported.[12−14] Cummins and co-workers reported a similar C_3-symmetric tris(anilido)Ti−oxo anion[15] and later reported reversible addition of CO_2 to this species to form a Ti-ligated carbonate.[16] Such a process seems relevant to our previously reported isolation of a Zr−carbonate species upon reduction of the CO_2 activation product (η^2-^{i}Pr$_2$PNMes)Zr(MesNP^{i}Pr$_2$)$_2$(μ-O)Co(CO).[8] In this article, the oxo anion [**2**]$^-$ is explored in more detail, looking at the effects of varying the countercation and exploring the reactivity of this species with electrophiles and additional CO_2 in the context of developing a potential catalytic cycle for CO_2 activation/functionalization involving the ZrCo tris(phosphinoamide) framework.

RESULTS AND DISCUSSION

The low yield (24%) of the anionic Zr−oxo species [**2**][**Na(THF)$_3$**][8] when generated by the reduction route shown in Scheme 1 necessitated that a new synthetic route be developed prior to studying its reactivity. An alternative synthesis began by adding excess carbon monoxide to **1** to give the diamagnetic complex (THF)Zr(MesNP^{i}Pr$_2$)$_3$Co(CO) (**3**) in 94% isolated yield (Scheme 2). The ^{31}P NMR spectrum

Scheme 2

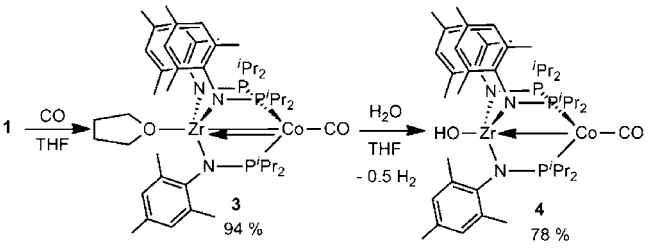

of **3** revealed a downfield shift to δ 60 ppm relative to the resonance of complex **1** at δ 35 ppm. The characteristic ν(CO) of **3** at 1890 cm^{-1} is similar to the carbonate species of similar Zr^{III}Co^0 oxidation state that we reported in an earlier publication (ν(CO) = 1884 cm^{-1}).[8] We note that assignment of formal oxidation states to each metal in complexes featuring metal−metal bonds is essentially meaningless, but this formalism is used herein to keep track of overall oxidation state. The one-electron reactivity that we previously encountered at Zr in two-electron-reduced species is consistent with the Zr^{III} oxidation state assignment.[17−19] We previously observed that backbonding from cobalt to a dinitrogen ligand is affected by the competitive Lewis acidity of zirconium and that this characteristic of the Zr/Co heterobimetallic system may be responsible for the remarkably high-energy stretching frequency of such highly reduced cobalt−carbonyls (Table 1).[11]

Table 1. Zr−Co Interatomic Distances and Infrared ν(CO) of XZr(MesNP^{i}Pr$_2$)$_3$Co(CO) Complexes of the Zr^{IV}Co^0 Oxidation State

compound	Zr−Co (Å)	ν(CO) (cm^{-1})
[**2**][**Li(THF)$_3$**]	2.5375(3)	1848,[a] 1855[b]
[**2**][**Li(12-c-4)**]	2.9236(3)	1843,[a] 1859[b]
[**2**][**Na(THF)$_3$**]	2.5333(5)	1853[b]
4	2.7486(6)	1893,[a] 1888[c]
5	2.7499(14)	1888[c]
6	2.7616(6)	1885[c]
7	2.7110(5)	1895[c]
[**8**][**K(18-c-6)**]	2.8468(5)	1875[c]
9	2.5965(4)	1904[c]

[a]IR spectrum measured in the solid state (KBr pellet). [b]IR spectrum measured in solution (THF). [c]IR spectrum measured in C_6H_6

The solid state structure of compound **3** was obtained via single-crystal X-ray diffraction (Figure S32, Supporting Information); however, repeated attempts to crystallize this compound resulted in a structure with THF/Cl disorder at the axial Zr position (a result of contamination with CH_2Cl_2 in the glovebox atmosphere over time), so rigorous conclusions about the interatomic distances in **3** cannot be drawn.

Addition of 1 equiv of H_2O to **3** at room temperature resulted in immediate evolution of gas and a color change of the reaction mixture from red to yellow (Scheme 2). The new compound had a ν(CO) of 1888 cm^{-1} (Table 1) and paramagnetically shifted resonances in its ^{1}H NMR spectrum (C_6D_6). In addition to the five resonances attributable to the tris(phosphinoamide) ligand framework, the ^{1}H NMR spectrum features a singlet at δ −41 ppm. A single-crystal X-ray diffraction study identified the new compound as the Zr−hydroxide compound (HO)Zr(MesNP^{i}Pr$_2$)$_3$Co(CO) (**4**, Figure 1). The resonance at δ −41 ppm in the ^{1}H NMR spectrum was assigned to the hydroxide proton. While this may seem like an unusual shift for a hydroxide proton, it is important to bear in mind that the hydroxide ligand is not directly bound to a paramagnetic metal center but is still influenced by the pendant paramagnetic Co ion. This gives rise to an unusual chemical shift, which can nonetheless be unambiguously assigned by comparison of the ^{1}H NMR spectrum of **4** with the ^{1}H NMR of a species obtained upon deprotonation (vide infra): These spectra are nearly identical, except for the absence of the δ −41 ppm resonance in the deprotonated complex. Further support for the assignment of **4** as a Zr−hydroxide complex is the O−H stretching modes present in the IR spectra in solution (C_6H_6, 3691 cm^{-1}) and solid state (3625 cm^{-1}). Compound **4** is formed in 78% yield and has an S = 1/2 ground state with μ_{eff} = 2.11 μ_B and can be assigned a Zr^{IV}Co^0 redox state. Compound **4** has a Zr−Co distance of 2.7486(6) Å and Zr−O bond distance of 1.909(2) Å. The Zr−Co distance in **4** is relatively long compared to both fully reduced Zr^{III}Co^0 complex **1** and the Zr^{IV}Co^I dihalide complex ClZr(MesNP^{i}Pr$_2$)$_3$CoI.[10,11] The Zr−O bond distance in **4** is shorter than that in other reported terminal Zr−hydroxides, such as structures reported by Parkin and co-workers with Zr−O bond distances of 2.010(2), 2.061(7), and 2.001 (6) Å.[20,21] The Zr-bound hydroxyl group is not engaged in any intermolecular hydrogen-bonding

dx.doi.org/10.1021/ic302473j | Inorg. Chem. 2013, 52, 3022−3031

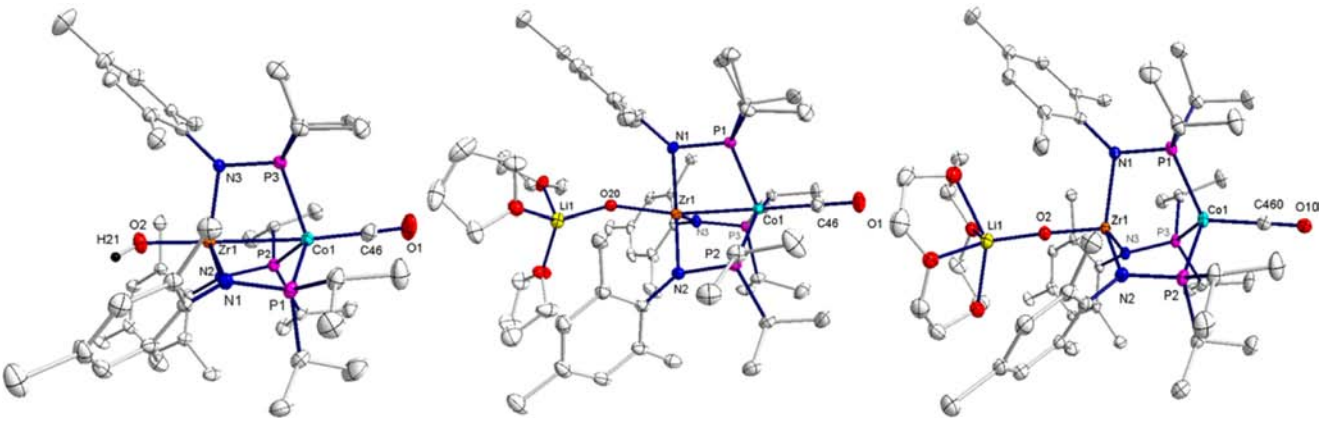

Figure 1. Displacement ellipsoid (50%) representations of **4** (left), [**2**][**Li**(**THF**)$_3$] (middle), and [**2**][**Li**(**12-c-4**)] (right). Hydrogen atoms except for H21 of **4** were omitted for clarity. Relevant interatomic distances (Angstroms) and angles (degrees). **4**: Zr−Co, 2.7486(6); Zr−O2, 1.909(2); Co−C46, 1.758(4); Co−Zr−O2, 179.32(8); Co−C46−O1, 178.6(4). [**2**][**Li**(**THF**)$_3$]: Zr−Co, 2.5375(3); Zr−O20, 2.130(6); Li−O20, 1.854(6); Co−C46, 1.7445(19); Co−Zr−O20, 169.0(2); Zr−O20−Li, 157.9(5); Co−C46−O1, 179.54(17). [**2**][**Li**(**12-c-4**)]: Zr−Co, 2.9236(3); Zr−O2, 1.8328(11); Li−O2, 1.806(3); Co−C460, 1.765(5); Co−Zr−O2, 178.24(4); Zr−O2−Li, 176.02(12); Co−C460−O10, 179.1(4).

interactions, presumably due to the steric constraints imposed by the bulky mesityl substituents. Structurally characterized terminal hydroxides are relatively uncommon, likely due to the ability of the hydroxide ligand to bridge two or more metal centers or the propensity of early metal hydroxides to undergo further reactivity leading to dimeric bridging oxo species.[22] The stability of the terminal hydroxide of compound **4** may be attributed to the steric bulk of the trisphosphinoamide ligand framework.

The reduced byproduct of the reaction to produce **4** from H_2O has been tentatively assigned as 0.5 equiv of H_2, as this assignment would be consistent with the gas that was evolved during reaction. A similar coupling of two methyl radicals extruded from a one-electron oxidation reaction of a Hf/Co complex with MeI to generate ethane has been reported and verified spectroscopically.[23] Structurally characterized Zr−hydroxide complexes have been synthesized by substitution reactions or addition of E−H bonds to a Zr−oxo species.[20−22,24−26] In a particularly relevant example, Rosenthal and co-workers report a reaction involving a Ti(III) starting material and water to produce 0.5 equiv of H_2 and a Ti^{IV}−hydroxide species.[27] In contrast, Zr(II) starting materials have been shown to react with 2 equiv of water to form a Zr−dihydroxide complex and 1 equiv of H_2.[21] The mechanisms of H_2 formation from the Ti(III) and Zr(II) starting materials differ in that the product from the Ti(III) starting material results from a hydrogen-atom transfer (HAT) mechanism,[27,28] whereas the Zr(II) starting material first reacts with 1 equiv of water to form a dimeric μ-O Zr−hydride species which subsequently reacts with a second equivalent of water to form the final Zr−dihydroxide species and 1 equiv of H_2.[26] At first glance, reaction of **3** with H_2O appears to be most closely related to reaction of the Ti(III) complex reported by Rosenthal, but we concede that an intermolecular mechanism involving a Zr−hydride or Co−hydride species cannot be ruled out at this time. The mechanism for this reaction and other E−H bond activations of this type by Zr/Co heterobimetallic complexes are discussed in more detail elsewhere.[17,18]

In an effort to generate a Zr−oxo anion from **4** via deprotonation, complex **4** was treated with 1 equiv of 1,8-diazabicycloundec-7-ene (DBU) in C_6D_6. If deprotonation had occurred we would expect the peak corresponding to the hydroxide proton to no longer appear in the resulting ^{1}H NMR spectrum (δ −41 ppm in C_6D_6 for **4**); however, after addition of DBU to **4** in C_6D_6, the resonance corresponding to the hydroxide proton remains but is shifted downfield to δ −33 ppm. This result led us to conclude that DBU is not a strong enough base to deprotonate the hydroxide ligand of **4** but that an intermolecular hydrogen-bonding interaction between DBU and the hydroxide proton leads to a shift in the latter's ^{1}H NMR signal. This prediction was supported by the solid state structure of **4·DBU** (Figure S36, Supporting Information), in which the proton associated with the hydroxide ligand was located in the difference map and found to be ∼1.8 Å from the basic DBU nitrogen atom. In light of this observation, a stronger base was chosen to deprotonate **4**.

To generate the desired anionic oxo species, complex **4** was treated with 1 equiv of lithium hexamethyldisilazide (LiN(SiMe$_2$)$_2$) (Scheme 3). Monitoring the progress of the reaction in THF-d_8 by ^{1}H NMR reveals loss of the resonance assigned to the proton for the hydroxide ligand at δ −33.7 ppm, while the remainder of the NMR resonances shift only slightly upon

Scheme 3

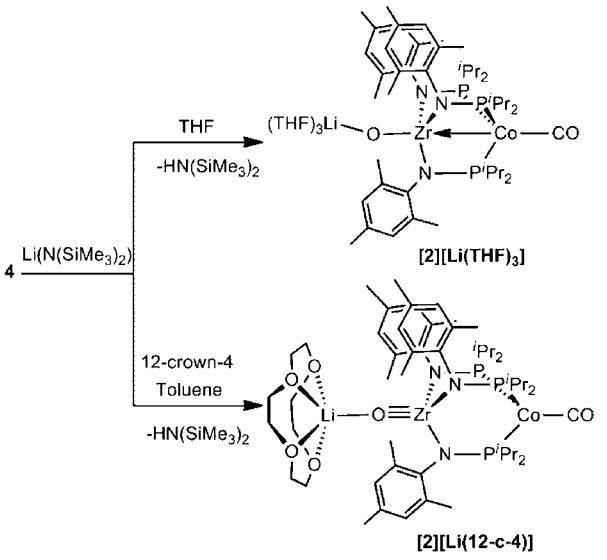

dx.doi.org/10.1021/ic302473j | Inorg. Chem. 2013, 52, 3022−3031

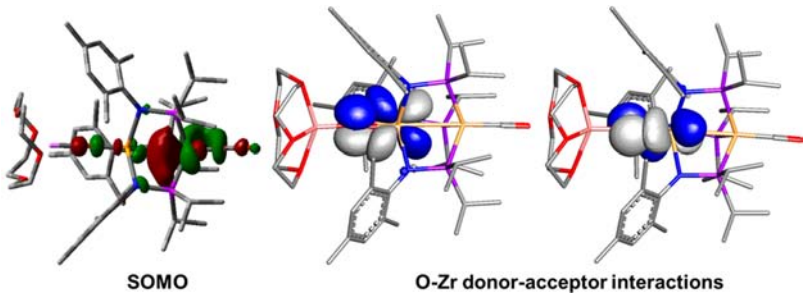

Figure 2. Calculated SOMO of [**2**][**Li(12-c-4)**] (left) and β-orbital-derived O to Zr donor−acceptor interactions obtained via NBO calculations (E_{del} = 16.3 and 14.7 kcal/mol, respectively). α-Orbital-derived O to Zr donor−acceptor interactions are included in the Supporting Information (BP86/LANL2TZ(f)/6-311G(d)/D95 V).

deprotonation. The structure of the new species was determined unambiguously by single-crystal X-ray diffraction to be [$(THF)_3$Li][OZr($MesNP^iPr_2$)$_3$Co(CO)] [**2**][**Li(THF)$_3$**] (Figure 1). The lithium countercation is associated with the disordered oxo atom, with distances ranging from 1.85 to 1.90 Å, and has three THF solvate molecules. In general, the structure bears close resemblance to that previously reported for [**2**][**Na(THF)$_3$**], except that the sodium ion also interacts with the π system of a mesityl substituent in the latter complex.[8] The oxygen atom bound to zirconium is disordered over three positions with bond distances ranging from 2.130(6) to 2.108(2) Å. In all three disordered positions, the Zr−O bond distance in [**2**][**Li(THF)$_3$**] is slightly longer than in [**2**][**Na(THF)$_3$**] (Zr−O bond distance = 2.071(2) Å)[8] and is also significantly longer than that in the Zr−oxo anion structure reported by Stephan (1.847(9) Å) or the neutral Zr−oxo structure reported by Parkin (1.804(4) Å).[12,24] In this context, it is also important to note that the Zr−Co distance (2.5375(3) Å) in [**2**][**Li(THF)$_3$**] is relatively short and indicative of a Zr−Co interaction. The relatively long Zr−O bond in [**2**][**Li(THF)$_3$**] appears to coincide with increased dative donation from Co to Zr.

In an attempt sequester the lithium cation, deprotonation of **4** with Li($N(SiMe_3)_2$) was performed in the presence of 12-crown-4 in toluene (Scheme 3). The solid state structure obtained via single-crystal X-ray diffraction revealed the formulation of the resulting complex to be [(12-crown-4)Li][OZr($MesNP^iPr_2$)$_3$Co(CO)] [**2**][**Li(12-c-4)**] (Figure 1). The crown ether did not sequester the lithium cation (even when excess crown ether was added); however, substantial structural changes occurred. The Zr−O distance of [**2**][**Li(12-c-4)**] is 1.8328(11) Å, which is ∼0.3 Å shorter than in [**2**][**Li(THF)$_3$**], and the Zr−Co distance is elongated to 2.9236(3) Å (compared to 2.5375(3) Å in [**2**][**Li(THF)$_3$**]). Another notable structural change is the contraction of the N−Zr−N bond angles to an average of 115.48(5)° for compound [**2**][**Li(12-c-4)**] from 119.05(6)° in [**2**][**Li(THF)$_3$**] as the Zr atom pushes out of the plane of the nitrogen donors to adopt a geometry closer to tetrahedral. The short Zr−O bond distance of [**2**][**Li(12-c-4)**] indicates an increase in the Zr−O bond order, and the local 3-fold symmetry at zirconium allows formation of one σ and two π bonds for a formal Zr−O bond order of three. Attempting to exchange the cation in [**2**][**Li(12-c-4)**] with a noncoordinating cation such as tetraethylammonium consistently resulted in a mixture of products, most notably reformation of compound **4**. Since tetraalkylammonium cations are known to undergo elimination in the presence of strong base, we attempted cation exchange with bis(triphenylphosphine)iminium ([PPN]$^+$); however, the PPN^+ cation did not appear to exchange with Li^+, indicating that the coordinating cation is necessary to stabilize the anionic Zr−oxo fragment.

Solution infrared spectra for compounds [**2**][**Li(THF)$_3$**] and [**2**][**Li(12-c-4)**] showed ν(CO) of 1855 (THF) and 1859 cm^{-1} (benzene), respectively (Table 1). These values are consistent with the previously reported ν(CO) for [**2**][**Na(THF)$_3$**] (1853 cm^{-1}).[8] The similarity of ν(CO) for these three compounds was unexpected based on the drastically different solid state structures, particularly since the stronger Zr−Co interaction in [**2**][**Li(THF)$_3$**] and [**2**][**Na(THF)$_3$**] would be expected to decrease the electron density on Co, leaving less electron density for backbonding with CO (leading to a higher energy CO stretch). To further investigate this phenomenon, solid state infrared spectra (KBr pellet) were collected for compounds [**2**][**Li(THF)$_3$**] and [**2**][**Li(12-c-4)**] and revealed ν(CO) of 1848 and 1843 cm^{-1}, respectively. The difference of only 5 cm^{-1} in the ν(CO) of compounds [**2**][**Li(THF)$_3$**] and [**2**][**Li(12-c-4)**] in the solid state suggests similar electronic structures for the two compounds and is not consistent with our observations that longer Zr−Co distances tend to correspond to lower ν(CO) (Table 1).

A computational investigation using density functional theory (DFT) was undertaken on the Li-capped anions [**2**][**Li(12-c-4)**] and [**2**][**Li(THF)$_3$**] to further probe their electronic structure and, in particular, to evaluate the Zr−O bond order. Using crystallographic coordinates as a starting point, geometry optimizations of both compounds using Gaussian09 (BP86/LANL2TZ(f)/6-311G(d)/D95 V)[29] resulted in nearly identical structures in stark contrast to the differences observed between these two compounds experimentally via X-ray crystallography (see Supporting Information). Both optimized geometries feature a short Zr−O distance (1.86 Å) and a long Zr−Co interatomic distance (2.95 Å), quite similar to the solid state Zr−O and Zr−Co distances in [**2**][**Li(12-c-4)**] (1.84 and 2.92 Å, respectively). The computed SOMOs of the $Zr^{IV}Co^0$ [**2**]$^-$ complexes clearly correspond to the Co d_{z^2} orbital and show essentially no interaction with the Zr center (since the two computed structures were nearly identical, we will limit our discussion to [**2**][**Li(12-c-4)**], whose SOMO is shown in Figure 2), as expected based on the long Zr−Co interatomic distance. Natural bond orbital (NBO)[30] analysis of [**2**][**Li(12-c-4)**] revealed two O→Zr donor−acceptor interactions corresponding to O−Zr π bonds (Figure 2), verifying the assignment as a triple-bonded Zr−oxo fragment. Moreover, the computed Zr−O Wiberg bond index (WBI) is 1.26,

dx.doi.org/10.1021/ic302473j | Inorg. Chem. 2013, 52, 3022−3031

corresponding to ~2.5 times the computed Zr−N single-bond WBI (~0.49).

When complexes [**2**][**Li(THF)$_3$**] and [**2**][**Li(12-c-4)**] were isolated and stored as solids at −35 °C for later use as a starting material, ^{1}H NMR spectra of the solids often contained mixtures of [**2**]$^-$ and **4** as a result of an unknown decomposition pathway. Due to the sensitivity of the Zr−oxo anion compounds, reactivity studies were performed by generating the Zr−oxo anion [**2**][**Li(12-c-4)**] in situ. Reactions of [**2**][**Li(12-c-4)**] with methyl trifluoromethanesulfonate (MeOTf) and timethylsilyl trifluoromethanesulfonate (TMSOTf) resulted in formation of the corresponding methoxide or trimethylsiloxide complexes (Scheme 4).

Scheme 4

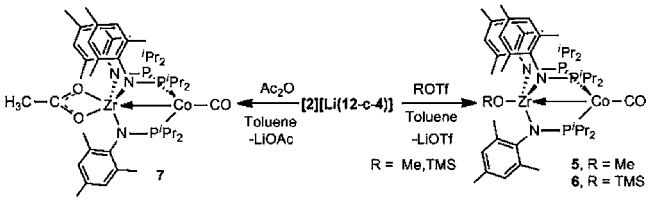

Compounds (MeO)Zr(MesNP^{i}Pr$_2$)$_3$Co(CO) (**5**) and (Me$_3$SiO)Zr(MesNP^{i}Pr$_2$)$_3$Co(CO) (**6**) have paramagnetically shifted ^{1}H NMR spectra with five resonances indicative of a Zr/Co system linked by three equivalent phosphinoamide ligands. The silyl methyl groups of **6** can be assigned to a resonance at 1.0 ppm in the ^{1}H NMR spectrum; however, the methyl protons of the methoxide ligand could not be located in the ^{1}H NMR spectrum of compound **5** and may be overlapping with a broad resonance belonging to a ligand signal. Solid state structures for compounds **5** and **6** were determined by single-crystal X-ray diffraction studies (Figure 3 and Figure S39, Supporting Information). The Zr−Co distances in structures **5** and **6** are 2.7499(14) and 2.7616(6) Å, respectively, with many of the structural features of **5** and **6** similar to those of hydroxide complex **4**. ν(CO) stretches of **5** and **6** are 1888 and 1885 cm^{-1}, respectively, in agreement with their closely related solid state structures (Table 1).

As shown in Scheme 4, reactivity of [**2**][**Li(12-c-4)**] with acetic anhydride (Ac$_2$O) also proceeds via electrophilic attack of the oxo anion to produce the corresponding lithium acetate salt and AcOZr(MesNP^{i}Pr$_2$)$_3$Co(CO) (**7**). The ^{1}H NMR spectrum of **7** contains a new resonance at δ 3.1 ppm assigned to the methyl group of the acetate ligand. Single-crystal X-ray diffraction studies show that the acetate ligand of **7** is bound in a κ^2-fashion (Figure 3). ν(CO) of **7** is at higher energy than **5** and **6** at 1895 cm^{-1} corresponding to a stronger Zr−Co interaction in **7**, which is further illustrated by a shorter Zr−Co distance of 2.7110(5) Å (Table 1).

Similar to the previously reported tris(anilide)Ti−oxo anion,[15,16] the Zr−oxo anion [**2**][**Li(12-c-4)**] also showed reactivity with 1 equiv of CO$_2$ (Scheme 5). The resulting product crystallizes from benzene as yellow prismatic crystals. The ^{1}H NMR spectrum of the crystals showed resonances for bound 12-crown-4, and the paramagnetically shifted peaks assigned to the trisphosphinoamide ligand resembled the pattern of **7** more closely than **5** or **6**, so the structure was tentatively assigned to be [(12-crown-4)Li][(κ^2-CO$_3$)Zr(MesNP^{i}Pr$_2$)$_3$Co(CO)] ([**8**][**Li(12-c-4)**]).

Compound [**8**][**Li(12-c-4)**] is soluble in pentane, making it difficult to isolate from any byproducts formed during the reaction, so the analogous complex with a potassium counter-cation and 18-crown-6 solvate, [**8**][**K(18-c-6)**], was synthesized via deprotonation of **4** with K(N(SiMe$_3$)$_2$) in the presence of 18-crown-6, followed by addition of 1 equiv of CO$_2$. Compound [**8**][**K(18-c-6)**] has ν(CO) = 1875 cm^{-1} and a correspondingly long Zr−Co distance of 2.8468(5) Å (Table 1, Figure 4). The IR spectrum of [**8**][**K(18-c-6)**] also contains an absorbance at 1642 cm^{-1} assigned to the carbonate ligand. When ^{13}CO$_2$ is used, the stretch assigned to the carbonate appears at 1600 cm^{-1} (calculated = 1605 cm^{-1}, see Supporting Information). Despite its paramagnetism (S = 1/2, μ_{eff} = 1.75 μ_B), the ^{13}C NMR spectrum of the ^{13}C-labeled carbonate complex [**8**][**K(18-c-6)**] shows a resonance at δ 158 ppm which is consistent with the value reported for the diamagnetic Ti−carbonate species at 160 ppm.[16]

Addition of CO$_2$ to the tris(anilide)Ti−oxo anion is reportedly reversible, with CO$_2$ binding being disfavored in the presence of strongly coordinating ethereal solvents.[16] While carbonate compound [**8**][**K(18-c-6)**] is stable as a solid at −35

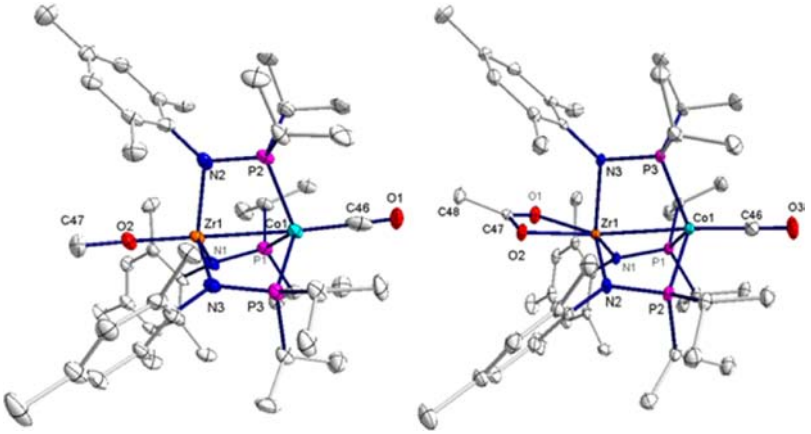

Figure 3. Displacement ellipsoid (50%) representations of **5** (left) and **7** (right). Hydrogen atoms were omitted for clarity. Relevant interatomic distances (Angstroms) and angles (degrees). **5**: Zr−Co, 2.7499(14); Zr−O2, 1.912(5); Co−C46, 1.815(12); Co−Zr−O2, 174.43(16); Zr−O2−C47, 168.5(6); Co−C46−O1, 178.1(9). **7**: Zr−Co, 2.7110(5); Zr−O1, 2.244(2); Zr−O2, 2.253(2); Co−C46−O3, 178.8(3), O1−C47−O2, 117.7(3).

dx.doi.org/10.1021/ic302473j | Inorg. Chem. 2013, 52, 3022−3031

Scheme 5

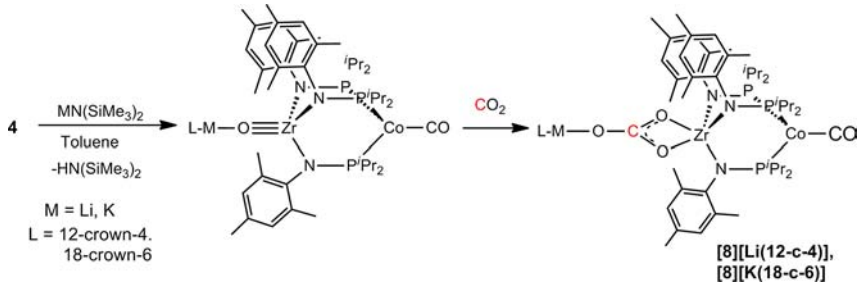

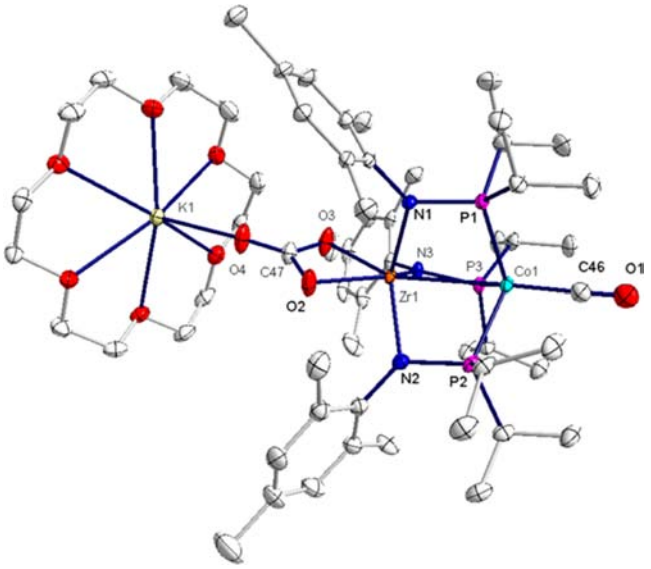

Figure 4. Displacement ellipsoid (50%) representations of [**8**][**K(18-c-6)**]. Hydrogen atoms were omitted for clarity. Relevant interatomic distances (Angstroms) and angles (degrees): Zr−Co, 2.8468(5); Zr−O2, 2.130(2); Zr−O3, 2.136(2); K−O4, 2.548(2); Co−C46, 1.750(4); O2−C47−O3, 110.6(3); K−O4−C47, 160.3(2); Co−C46−O1, 176.5(4).

°C for more than 1 month with no signs of decomposition, we observed decomposition of approximately 50% of [**8**][**K(18-c-6)**] to **4** and free phosphinoamine ligand in solution after 5 days by ^{1}H NMR spectroscopy. Formation of **4** from [**8**][**K(18-c-6)**] indicates that carbonate formation may also be reversible in this system. When excess CO_2 was added to ^{13}C-labeled carbonate product [**8**][**K(18-c-6)**] in a J-Young NMR tube, the resonance assigned to the carbonate moiety at 158 ppm in the ^{13}C NMR spectrum disappeared and was replaced by a new resonance at 125 ppm assigned to free $^{13}CO_2$ (see Supporting Information). A solution IR spectrum of the isolated solid from this reaction confirmed that unlabeled CO_2 displaced the labeled $^{13}CO_2$, as a strong absorbance reappeared at 1642 cm^{-1}. Notably, prolonged exposure of [**8**][**K(18-c-6)**] to dynamic vacuum did not lead to detectable CO_2 loss to regenerate the oxo species or hydroxo complex **4**.

Previously, we reported that the CO_2 activation product (η^2-$^{i}Pr_2$PNMes)Zr(MesNP^{i}Pr$_2$)$_2$(μ-O)Co(CO) can be reduced with excess Na/Hg to afford the two-electron-reduced Zr−carbonate species [(THF)$_2$Na]$_2$(CO$_3$)Zr(MesNP^{i}Pr$_2$)$_3$Co(CO). This product is formed in high yield in the presence of an additional equivalent of CO_2; however, it also forms in ∼40% yield when no external CO_2 is added. The mechanism by which carbonate formation occurs in the absence of added CO_2 remains unclear, and addition of CO to oxo anion [**2**]$^-$ results in no apparent reaction (although a reversible reaction to generate CO_2 cannot be ruled out at this time). However, the reactivity of oxo anion [**2**]$^-$ with CO_2 to form carbonate [**8**]$^-$ lends insight into carbonate formation under reductive conditions in the presence of exogenous CO_2. Once a one-electron reduction of (η^2-$^{i}Pr_2$PNMes)Zr(MesNP^{i}Pr$_2$)$_2$(μ-O)-Co(CO) occurs to form an anionic oxo such as [**2**]$^-$, CO_2 can bind to form an S = 1/2 carbonate species such as [**8**]$^-$. Additional one-electron reduction of this complex would lead to formation of the diamagnetic carbonate complex [(THF)$_2$Na]$_2$(CO$_3$)Zr(MesNP^{i}Pr$_2$)$_3$Co(CO). Indeed, cyclic voltammetry of [**8**][**K(18-c-6)**] shows a reversible reductive feature around −2.0 V (see Supporting Information).

With some reactivity for [**2**][**Li(12-c-4)**] established we set out to complete a hypothetical synthetic cycle for reduction of CO_2. One such synthetic cycle was reported by Donahue and co-workers regarding a W(II/IV) cycle for CO_2 reduction to CO.[31] As shown in Scheme 6a, addition of 1 equiv of HCl to

Scheme 6

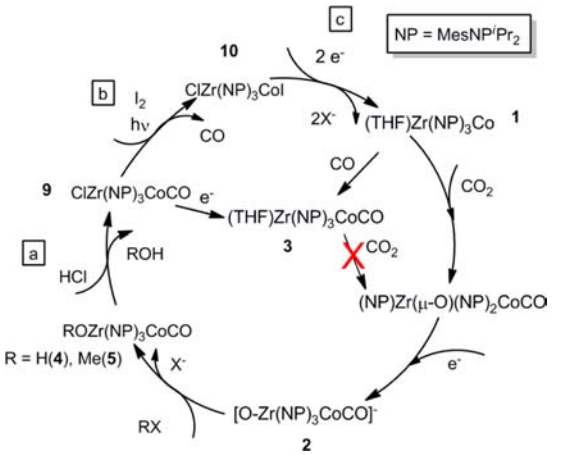

either the hydroxide complex **4** or the methoxide complex **5** affords ClZr(MesNP^{i}Pr$_2$)$_3$Co(CO) (**9**) with concomitant release of H_2O or MeOH. In the case of **5**, methanol was detected in the ^{1}H NMR spectrum of the volatiles from this reaction as a singlet at δ 3.07 ppm (see Supporting Information). Compound **9** was isolated in 78% yield and crystallized from diethyl ether to provide red-orange X-ray-quality crystals (Figure S45, Supporting Information). ν(CO) for **9** of 1905 cm^{-1} is consistent with weaker back-bonding from Co to CO and thus a shorter Zr−Co distance (2.5965(4) Å). Compound **9** can be rereduced to **3** using Na/Hg amalgam; however, **3** does not react in the same manner as **1** with CO_2 to

dx.doi.org/10.1021/ic302473j | Inorg. Chem. 2013, 52, 3022−3031

afford (η^2-^{i}Pr$_2$PNMes)Zr(MesNP^{i}Pr$_2$)$_2$(μ-O)Co(CO), falling short of a completed cycle for CO_2 reduction. Thus, to reform **1** and complete a hypothetical cycle, compound **9** was photolyzed in the presence of I_2 to regenerate ClZr(MesNP^{i}Pr$_2$)$_3$CoI (**10**) in 67% isolated yield (Scheme 6b). Formation of complex **1** from compound **10** was previously shown to proceed readily via reduction (Scheme 6c).[10,11]

CONCLUSIONS

In summary, the reactivity of an unusual anionic Zr−oxo species toward electrophiles and CO_2 has been investigated. In order to study this reactivity, an alternative high-yielding synthesis of the Zr−oxo anion species has been devised. This synthetic route involves formation of a terminal Zr−hydroxide via a one-electron oxidation of **3** by H_2O, extruding H_2. Deprotonation of the Zr−hydroxide species using Li(N(SiMe$_3$)$_2$) provides an anionic Zr−oxo species similar to that previously reported. Interestingly, we found that many of the structural features, including Zr−Co distance and Zr−O distance, of these heterobimetallic species in the solid state were highly dependent on the solvation of the alkali countercation. Nonetheless, the solution behavior (spectroscopy and reactivity) of these complexes did not seem to vary with counterion. In general, multiple bonding between the oxo ligand and Zr appears to weaken the dative interaction between Zr and Co, as evident by elongated metal−metal separations and increased Co−CO back-bonding.

The Zr−oxo anion reacts readily with electrophiles such as Me^+, Me_3Si^+, and Ac_2O to form zirconium methoxide, siloxide, and acetate products, respectively. An additional equivalent of CO_2 also reacts with the anionic oxo fragment to generate a Zr−carbonate anion. Carbonate formation is apparently reversible, as elucidated through exchange between isotopically labeled $^{13}CO_2$ and CO_2 in this carbonate species. Lastly, we demonstrated that the oxoanion can be converted, albeit through a series of stoichiometric steps, back to a complex capable of activating additional CO_2. The fundamental reaction steps examined herein are of relevance to the electrochemical reduction of CO_2, namely, the steps required to functionalize and cleave strong early metal−oxygen linkages. Future studies will focus on investigations into realizing a true catalytic cycle for CO_2 reduction using these heterobimetallic Zr/Co complexes and other heterobimetallic combinations.

EXPERIMENTAL SECTION

General Considerations. Unless specified otherwise, all manipulations were performed under an inert atmosphere using standard Schlenk or glovebox techniques. Glassware was oven dried before use. Benzene, pentane, diethyl ether, tetrahydrofuran, and toluene were dried using a Glass Contours drying column. All solvents were stored over 3 Å molecular sieves. Benzene-d_6 and toluene-d_8 (Cambridge Isotopes) were degassed via repeated freeze−pump−thaw cycles and dried over 3 Å molecular sieves. THF-d_8 was dried over CaH_2, vacuum transferred, and degassed via repeated freeze−pump−thaw cycles. (THF)Zr(MesNP^{i}Pr$_2$)$_3$CoN$_2$ was synthesized using literature procedures.[11] Carbon dioxide (bone dry grade 3.0) and carbon monoxide (CP grade 2.5) were purchased from Airgas and used without further purification. All other chemicals were purchased from commercial vendors and used without further purification. For ^{1}H and ^{13}C NMR spectra the solvent resonance was referenced as an internal standard, and for ^{31}P{^{1}H} NMR spectra the 85% H_3PO_4 resonance was referenced as an external standard. IR spectra were recorded on a Varian 640-IR spectrometer controlled by Resolutions Pro software. UV−vis spectra were recorded on a Cary 50 UV−vis spectrophotometer using Cary WinUV software. Elemental analyses were performed at Complete Analysis Laboratory Inc., Parsippany, NJ. Solution magnetic moments were measured using Evans' method and are reported without taking into account any diamagnetic contributions (Pascal's constants were not used).[32,33]

X-ray Crystallography Procedures. All operations were performed on a Bruker-Nonius Kappa Apex2 diffractometer using graphite-monochromated Mo Kα radiation. All diffractometer manipulations, including data collection, integration, scaling, and absorption corrections, were carried out using the Bruker Apex2 software.[34] Preliminary cell constants were obtained from three sets of 12 frames. Fully labeled diagrams and data collection and refinement details are included in Tables S1−S3 and on pages S23−S46 of the Supporting Information file. Further crystallographic details may be found in the accompanying CIF files.

Computational Details. All calculations were performed using Gaussian09, Revision A.02 for the Linux operating system.[29] Density functional theory calculations were carried out using a combination of Becke's 1988 gradient-corrected exchange functional[35] and Perdew's 1986 electron correlation functional[36] (BP86). A mixed basis set was employed using the LANL2TZ(f) triple-ζ basis set with effective core potentials for cobalt and zirconium,[37] Gaussian09's internal 6-311+G(d) for heteroatoms (nitrogen, oxygen, phosphorus), and Gaussian09's internal LANL2DZ basis set (equivalent to D95V[38]) for carbon and hydrogen. Using crystallographically determined geometries as a starting point, geometries were optimized to a minimum, followed by analytical frequency calculations to confirm that no imaginary frequencies were present.

Electrochemistry. Cyclic voltammetry measurements were carried out in a glovebox under a dinitrogen atmosphere in a one-compartment cell using a CH Instruments electrochemical analyzer. A glassy carbon electrode and platinum wire were used as the working and auxiliary electrodes, respectively. The reference electrode was Ag/AgNO$_3$ in THF. Solutions (THF) of electrolyte (0.40 M [nBu$_4$N][PF$_6$]) and analyte (2 mM) were also prepared in the glovebox.

(THF)Zr(MesNP^{i}Pr$_2$)$_3$Co(CO) (3). A solution containing 0.6283 g (0.6275 mmol) of (N$_2$)Co(^{i}Pr$_2$PNMes)$_3$ZrTHF in THF (40 mL) was charged to a Schlenk tube containing a stir bar and sealed with a Teflon valve. Approximately one-half of the volatiles were removed in vacuo, resulting in a color change from the red N$_2$-ligated species to the blue/green **1**. The reaction vessel was resealed, frozen, and backfilled with excess CO(g). As the solution thawed and began stirring it turned to a red/orange color. The solution was allowed to stir for 10 min before being refrozen and evacuated. After thawing the reaction mixture, volatiles were removed in vacuo until about 10 mL of the reaction mixture remained. The THF solution was transferred to a scintillation vial, and volatiles were removed, yielding an analytically pure red/orange solid (0.5875 g, 93.57%). X-ray-quality red crystals were grown from concentrated diethyl ether at −35 °C; however, in all cases these crystals were contaminated with **9** (Cl^- likely resulted from contamination with CH_2Cl_2 in the glovebox atmosphere over time). Repeated careful attempts to crystallize **3** in the absence of any Cl^- contamination did not result in any crystals suitable for X-ray diffraction. ^{1}H NMR (400 MHz, C_6D_6): δ 6.77 (s, 6H, Mes), 2.73 (m, 6H, CH(CH$_3$)$_2$), 2.57 (m, 4H, THF), 2.47 (s, 18H, Mes-Me), 2.13 (s, 9H, Mes-Me), 1.85 (m, 18H, CH(CH_3)$_2$), 1.53 (m, 18H, CH(CH_3)$_2$), 0.56 (m, 4H, THF). ^{31}P NMR (162 MHz, C_6D_6): δ 60 (very broad). ^{13}C NMR (100.5 MHz, C_6D_6): δ 149.0 (*ipso*-Mes), 134.5 (Mes), 131.0 (Mes), 129.1(Mes), 69.1 (THF), 44.2 (PC(CH$_3$)$_2$), 24.9 (THF), 24.2 (PC(CH_3)$_2$), 23.0 (PC(CH_3)$_2$, 23.2 Mes-Me, 20.7 (Mes-Me). IR (THF): 1890 cm^{-1}. UV−vis (C_6H_6, λ(nm) (ε, M^{-1} cm^{-1}): 364 (sh), 456 (640), 510 (270), 1021 (110). Anal. Calcd for $C_{50}H_{83}CoN_3O_2P_3Zr$: C, 59.98; H, 8.36; N, 4.20. Found: C, 59.82; H, 8.19; N, 4.14.

(HO)Zr(MesNP^{i}Pr$_2$)$_3$Co(CO) (4). A solution containing 0.5777 g (0.5769 mmol) of **3** in THF (10 mL) was charged to a Schlenk tube containing a stir bar and sealed with a Teflon valve. A 5 mL (0.5950 mmol) amount of a 0.119 M solution of H_2O in THF, prepared from 107 μL of N$_2$-sparged deionized water and 50 mL of THF, was added dropwise via a syringe to the stirring solution of **3** in THF. The

dx.doi.org/10.1021/ic302473j | Inorg. Chem. 2013, 52, 3022−3031

reaction mixture was allowed to stir for 15 min, during which time gas was evolved and the color of the solution changed from red to yellow. The reaction mixture was transferred to a scintillation vial, and volatiles were removed. The remaining yellow solid was washed with cold pentane to yield an analytically pure solid (0.4251 g, 77.9%). Yellow X-ray-quality crystals were grown in concentrated diethyl ether at room temperature. ^{1}H NMR (400 MHz, C_6D_6): δ 8.2 (s, 6H, Mes-Ar), 5.5 (br s, 18H, CH(CH_3)$_2$), 3.1 (br s, 18H, CH(CH_3)$_2$), 2.3 (s, 18H, Mes-Me), −2.8 (br s, 9H, Mes-Me), −40.6 (s, 1H, O*H*). ^{1}H NMR (400 MHz, THF-d_8): 8.0 (s, 6H, Mes-Ar), 5.3 (br s, 18H, CH(CH_3)$_2$), 3.0 (br s, 18H, CH(CH_3)$_2$), 2.2 (s, 18H, Mes-Me), −2.9 (br s, 9H, Mes-Me), −33.7 (s, 1H, O*H*). IR (C_6H_6): 3690 cm^{-1}(O−H), 1888 cm^{-1}(CO). KBr pellet: 3624 cm^{-1} (O−H), 1893 cm^{-1} (CO). UV−vis (C_6H_6, λ(nm) (ε, M^{-1} cm^{-1}): 498 (520), 689 (220), 1045 (300). Evans' method (μ_{eff}, C_6D_6): 2.11 μ_B. Anal. Calcd for $C_{46}H_{76}N_3O_2P_3ZrCo$: C, 58.39; H, 8.10; N, 4.44. Found: C, 58.30; H, 8.14; N, 4.39.

DBU-HOZr(MesNP^{i}Pr$_2$)$_3$Co(CO) (4·DBU). A solution containing 0.0389 g (0.0411 mmol) of **4** in C_6H_6 (2 mL) was prepared in a scintillation vial containing a stir bar. A solution containing 6.4 μL (0.043 mmol) of 1,8-diazabicycloundec-7-ene (DBU) in C_6H_6 was added to the solution of **4** dropwise. The reaction mixture was allowed to stir for 15 min, and volatiles were removed in vacuo. Pentane was added to the remaining yellow-orange solid and placed in the freezer at −35 °C. After 24 h, the supernatant was decanted and the resulting solid was dried in vacuo to give **4·DBU** as an analytically pure yellow-orange solid (0.0435 g, 96.3%). Yellow-orange X-ray-quality crystals were grown from a concentrated solution of diethyl ether at room temperature. ^{1}H NMR (400 MHz, C_6D_6): δ 8.2 (s, 6H, Mes-Ar), 5.4 (br s, 18H, CH(CH_3)$_2$), 3.6 (DBU), 3.1 (br s, 18H, CH(CH_3)$_2$), 2.9 (DBU), 2.8 (DBU), 2.7 (DBU), 2.3 (s, 18H, Mes-Me),1.8 (DBU), 1.5 (DBU), 1.3 (DBU), −2.8 (br s, 9H, Mes-Me), −33.0 (s, 1H, O*H*). IR (C_6H_6): 1886 cm^{-1}. UV−vis (C_6H_6, λ(nm) (ε, M^{-1} cm^{-1}): 367 (sh), 509 (200), 1027 (240). Evans' method (μ_{eff}, C_6D_6): 2.11 μ_B Anal. Calcd for $C_{55}H_{92}N_5O_2P_3CoZr$: C, 60.14; H, 8.44; N, 6.38. Found: C, 59.97; H, 8.62; N, 6.42.

[(THF)$_3$Li][OZr(MesNP^{i}Pr$_2$)$_3$Co(CO)] [2][Li(THF)$_3$]. Lithium hexamethyldisilazide 0.0064 g (0.038 mmol) was dissolved in THF (1 mL) and frozen in a scintillation vial containing a stir bar. A separate solution containing 0.0350 g (0.0370 mmol) of **4** in THF (2 mL) was cooled to near freezing and pipetted onto the frozen solution of LiHMDS. The reaction mixture was allowed to stir for 5 min while warming to room temperature. The reaction mixture was filtered, concentrated, and layered with pentane for crystallization at room temperature. After 24 h, the orange X-ray-quality crystals (0.0219 g, 50.7%) were isolated from the mother liquor. ^{1}H NMR (400 MHz, THF-d_8): δ 7.6 (s, 6H, Mes-Ar), 5.0 (br s, 18H, CH(CH_3)$_2$), 3.6 (THF), 3.2 (br s, 18H, CH(CH_3)$_2$), 2.2 (s, 9H, Mes-Me), 1.7 (THF) −3.5 (br s, 18H, Mes-Me). IR (THF-d_8): 1855 cm^{-1}. KBr pellet: 1848 cm^{-1}. UV−vis (THF, λ(nm) (ε, M^{-1} cm^{-1}): 366 (sh), 506 (500), 1042 (190). Anal. Calcd for $C_{58}H_{99}LiN_3O_5P_3ZrCo$: C, 59.62; H, 8.54; N, 3.60. Found: C, 59.51; H, 8.59; N, 3.70.

[(12-crown-4)Li][OZr(MesNP^{i}Pr$_2$)$_3$Co(CO)] [2][Li(12-c-4)]. A solution containing 20.6 μL (0.1271 mmol) of 12-crown-4 and 0.0217 g (0.1297 mmol) of lithium hexamethyldisilazide in toluene (3 mL) was cooled in a scintillation vial along with a separate solution of 0.1167 g (0.1235 mmol) of **4** in toluene (3 mL) in a scintillation vial containing a stir bar. The cold solution containing LiHMDS/12-crown-4 was added dropwise to the stirring, cold solution of **4**. The reaction mixture was stirred 10 min. Volatiles were removed in vacuo. The remaining yellow solid was washed with cold pentane, giving the product (0.1073 g, 77.04%). Yellow X-ray-quality crystals were grown in concentrated diethyl ether at room temperature. ^{1}H NMR (400 MHz, C_6D_6): δ 7.9 (s, 6H, Mes-Ar), 5.3 (br s, 18H, CH(CH_3)$_2$), 4.3 (8H, 12-Crown-4), 3.5 (overlap, 12-Crown-4), 3.4 (br s, overlap, CH(CH_3)$_2$), 2.3 (s, 9H, Mes-Me), 0.50 (br, 6H, C*H*(CH_3)$_2$), −3.3 (br s, 18H, Mes-Me). IR (C_6H_6): 1859 cm^{-1}. KBr pellet: 1843 cm^{-1}. UV−vis (C_6H_6, λ(nm) (ε, M^{-1} cm^{-1}): 367 (sh), 466 (sh), 505 (320). Evans' method (μ_{eff}, C_6D_6): 1.92 μ_B Anal. Calcd for $C_{54}H_{91}LiN_3O_6P_3ZrCo$: C, 57.48; H, 8.13; N, 3.72. Found: C, 57.43; H, 8.23; N, 3.70.

(MeO)Zr(MesNP^{i}Pr$_2$)$_3$Co(CO) (5). A solution containing 8.7 μL (0.054 mmol) of 12-crown-4 and 0.0090 g (0.054 mmol) of lithium hexamethyldisilazide in toluene (2 mL) was cooled in a scintillation vial along with a separate solution of 0.0460 g (0.0486 mmol) of **4** in toluene (2 mL) in a scintillation vial containing a stir bar. The cold solution containing LiHMDS/12-crown-4 was added dropwise to the stirring, cold solution of **4**. The reaction mixture was stirred 10 min before another cold solution of 5.5 μL (0.050 mmol) of MeOTf in toluene (1 mL) was added dropwise to the stirring reaction mixture. Volatiles were removed from the reaction mixture in vacuo. Remaining solid was extracted into ether, and again, volatiles were removed in vacuo, giving an analytically pure yellow solid (0.0372 g, 79.7%). Yellow X-ray-quality crystals were grown in concentrated diethyl ether at room temperature. ^{1}H NMR (400 MHz, C_6D_6): δ 8.3 (s, 6H, Mes-Ar), 5.5 (br s, 18H, CH(CH_3)$_2$), 3.1 (br s, 18H, CH(CH_3)$_2$), 2.3 (s, 9H, Mes-Me), −2.8 (br s, 18H, Mes-Me). IR (C_6H_6): 1888 cm^{-1}. UV−vis (C_6H_6, λ(nm) (ε, M^{-1} cm^{-1}): 366 (sh), 505 (240), 1027 (280). Evans' method (μ_{eff}, C_6D_6): 1.96 μ_B Anal. Calcd for $C_{47}H_{78}N_3P_3ZrCoO_2$: C, 58.79; H, 8.19; N, 4.38. Found: C, 58.68; H, 8.06; N, 4.29.

(Me$_3$SiO)Zr(MesNP^{i}Pr$_2$)$_3$Co(CO) (6). A solution containing 4.0 μL (0.025 mmol) of 12-crown-4 and 0.0041 g (0.025 mmol) of lithium hexamethyldisilazide in toluene (2 mL) was cooled in a scintillation vial along with a separate solution of 0.0211 g (0.0223 mmol) of **4** in toluene (2 mL) in a scintillation vial containing a stir bar. The cold solution containing LiHMDS/12-crown-4 was added dropwise to the stirring, cold solution of **4**. The reaction mixture was stirred 10 min before another cold solution of 4.2 μL (0.023 mmol) of TMSOTf in toluene (1 mL) was added dropwise to the stirring reaction mixture. Volatiles were removed from the reaction mixture in vacuo. The remaining solid was extracted into ether, and again the volatiles were removed in vacuo, giving an analytically pure yellow solid (0.0187 g, 82.5%). Yellow, rhombohedral X-ray-quality crystals were grown from diethyl ether at −35 °C. ^{1}H NMR (400 MHz, C_6D_6): δ 8.2 (s, 6H, Mes-Ar), 5.6 (br s, 18H, CH(CH_3)$_2$), 3.1 (br s, 18H, CH(CH_3)$_2$), 2.3 (s, 9H, Mes-Me), 1.0 (s, 9H, Si(CH_3)$_3$), −2.7 (br s, 18H, Mes-Me). IR (C_6H_6): 1885 cm^{-1}. UV−vis λ(nm) (ε, M^{-1} cm^{-1}): 504 (550), 687 (200), 1040 (230). Evans' method (μ_{eff}, C_6D_6): 2.37 μ_B Anal. Calcd for $C_{49}H_{84}N_3P_3ZrCoSiO_2$: C, 57.79; H, 8.31; N, 4.13. Found: C, 57.84; H, 8.25; N, 4.02.

(κ^2-AcO)Zr(MesNP^{i}Pr$_2$)$_3$Co(CO) (7). A solution containing 10.8 μL (0.0667 mmol) of 12-crown-4 and 0.0111 g (0.0667 mmol) of lithium hexamethyldisilazide in toluene (2 mL) was cooled in a scintillation vial along with a separate solution of 0.0573 g (0.0606 mmol) of **4** in toluene (2 mL) in a scintillation vial containing a stir bar. The cold solution containing LiHMDS/12-crown-4 was added dropwise to the stirring, cold solution of **4**. The reaction mixture was stirred 10 min before another cold solution of 5.9 μL (0.062 mmol) of acetic anhydride in toluene (1 mL) was added dropwise to the stirring reaction mixture. Volatiles were removed from the reaction mixture in vacuo. The remaining solid was extracted into pentane, concentrated, and placed in a −35 °C freezer. After 24 h X-ray-quality orange crystals were isolated (0.0393 g, 65.6%) by decanting the remaining pentane solution. ^{1}H NMR (400 MHz, C_6D_6): δ 8.4 (s, 6H, Mes-Ar), 5.9 (br s, 18H, CH(CH_3)$_2$), 3.1 (s, 3H, C(O)C*H*$_3$), 2.8 (br s, 18H, CH(CH_3)$_2$), 2.1 (s, 9H, Mes-Me), −2.0 (br s, 18H, Mes-Me). IR (C_6H_6): 1895 cm^{-1}. UV−vis (C_6H_6, λ(nm) (ε, M^{-1} cm^{-1}): 448 (800), 511 (230), 1011 (200). Evans' method (μ_{eff}, C_6D_6): 1.83 μ_B Anal. Calcd for $C_{48}H_{78}N_3O_3P_3CoZr$: C, 58.34; H, 7.96; N, 4.25. Found: C, 58.29; H, 8.03; N, 4.16.

[(12-Crown-4)Li][(CO_3-κ^2)Zr(MesNP^{i}Pr$_2$)$_3$Co(CO)] [8][Li(12-c-4)]. A solution containing 8.4 μL (0.052 mmol) of 12-crown-4 and 0.0087 g (0.052 mmol) of lithium hexamethyldisilazide in benzene (2 mL) was cooled in a scintillation vial along with a separate solution of 0.0470 g (0.0497 mmol) of **4** in benzene (2 mL) in a scintillation vial containing a stir bar. The cold solution containing LiHMDS/12-crown-4 was added dropwise to the stirring, cold solution of **4**. The reaction mixture and stir bar were transferred to a Schlenk tube and

dx.doi.org/10.1021/ic302473j | Inorg. Chem. 2013, 52, 3022−3031

sealed with a Teflon valve. After the reaction stirred for 10 min, the solution was frozen and then the headspace of the flask was evacuated and backfilled with 1.25 equiv of CO_2 using a known-volume gas bulb and partial pressure methods. After stirring for 15 min, the reaction mixture was filtered, concentrated, and allowed to crystallize at room temperature. After 24 h the mixture of crystals containing the product and **4** were washed with ether to leave an analytically pure orange solid (0.0108 g, 18.6%). ^{1}H NMR (400 MHz, C_6D_6): δ 8.3 (s, 6H, Mes-Ar), 5.6 (br s, 18H, $CH(CH_3)_2$), 3.8 (s, 16H, 12-crown-4), 3.1 (br s, 18H, $CH(CH_3)_2$), 2.3 (s, 9H, Mes-Me), −2.0 (br s, 18H, Mes-Me). IR (C_6H_6): 1885 cm^{-1}. UV−vis (C_6H_6, λ(nm) (ε, M^{-1} cm^{-1})): 508 (90), 1018 (120). Evans' method (μ_{eff}, C_6D_6): 2.04 μ_B Anal. Calcd for $C_{55}H_{91}O_8N_3P_3ZrCoLi$: C, 56.35; H, 7.82; N, 3.58. Found: C, 56.41 H, 7.92; N, 3.54.

[(18-Crown-6)K][(κ^2-CO_3)Zr(MesNP^{i}Pr$_2$)$_3$Co(CO) [8][K(18-c-6)]. A solution containing 0.0174 g (0.0658 mmol) of 18-crown-6 and 0.0131 g (0.0658 mmol) of potassium hexamethyldisilazide in toluene (2 mL) was cooled in a scintillation vial along with a separate solution of 0.0593 g (0.0627 mmol) of **4** in toluene (3 mL) in a scintillation vial containing a stir bar. The cold solution containing KHMDS/18-crown-6 was added dropwise to the stirring, cold solution of **4**. The reaction mixture and stir bar were transferred to a Schlenk tube and sealed with a Teflon valve. After the reaction stirred for 10 min, the solution was frozen and then the headspace of the flask was evacuated and backfilled with 1.25 equiv of CO_2 using a known-volume gas bulb and partial pressure methods. After stirring for 15 min, the reaction mixture was filtered and volatiles were removed in vacuo. The remaining solid was washed with pentane, leaving a yellow analytically pure solid (0.0422 g, 52.1%). ^{1}H NMR (400 MHz, C_6D_6): δ 8.0 (s, 6H, Mes-Ar), 5.9 (br s, 18H, $CH(CH_3)_2$), 3.6 (s, 24H, 18-crown-6), 2.9 (br s, 18H, $CH(CH_3)_2$), 2.1 (s, 9H, Mes-Me), −2.2 (br s, 18H, Mes-Me). IR (C_6H_6): 1875 cm^{-1}. UV−vis (C_6H_6, λ(nm) (ε, M^{-1} cm^{-1}): 510 (290), 1001 (200). Evans' method (μ_{eff}, C_6D_6): 1.75 μ_B Anal. Calcd for $C_{59}H_{99}N_3O_{10}KP_3CoZr$: C, 54.82; H, 7.72; N, 3.25. Found: C, 54.77; H, 7.64; N, 3.25.

ClZr(MesNP^{i}Pr$_2$)$_3$Co(CO) (9) from 5. A solution containing 0.0089 g (0.0093 mmol) of **5** in C_6D_6 was added to a J-Young NMR tube. A 9.9 μL (0.0099 mmol) amount of a 1 M HCl/ether solution was added to the C_6D_6 solution of **5**. After mixing, the solution changed from yellow to orange. Volatiles of the reaction mixture were transferred to a separate J-Young NMR tube. The orange solid was extracted into diethyl ether. Volatiles were removed in vacuo, leaving an analytically pure yellow/orange solid (0.0070 g, 78%). Red-orange X-ray-quality crystals were grown from a concentrated diethyl ether solution at −35 °C over 24 h. ^{1}H NMR (400 MHz, C_6D_6): δ 8.4 (s, 6H, Mes-Ar), 5.3 (br s, 18H, $CH(CH_3)_2$), 3.9 (br, 6H, $CH(CH_3)_2$), 3.0 (br s, 18H, $CH(CH_3)_2$), 2.3 (s, 9H, Mes-Me), −2.3 (br s, 18H, Mes-Me). IR (C_6H_6): 1904 cm^{-1}. UV−vis (C_6H_6, λ(nm) (ε, M^{-1} cm^{-1})): 403 (sh), 1025 (310). Evans' method (μ_{eff}, C_6D_6): 1.81 μ_B Anal. Calcd for $C_{46}H_{75}N_3OCl\ P_3CoZr$: C, 57.27; H, 7.84; N, 4.36. Found: C, 56.98; H, 7.91; N, 4.11. Formation of MeOH was confirmed by the presence of a singlet at 3.07 ppm in the proton NMR of the volatiles from the reaction mixture.

ClZr(MesNP^{i}Pr$_2$)$_3$CoI (10). A solution containing 0.0152 g (0.0158 mmol) of **9** in C_6D_6 was added to a J. Young NMR tube. Another solution containing 0.0022 g (0.0087 mmol) of I_2 in C_6D_6 was added to the J. Young tube. The J. Young tube was irradiated with 300 nm light (Rayonet RPR 3000 Å bulbs) for 3 h 45 min. The reaction mixture was a brown-green solution. The reaction mixture was filtered, and the volatiles were removed in vacuo. Remaining solids were washed with pentane, leaving a green solid (0.0113 g, 67.1%), which was identified by comparison of its ^{1}H NMR spectrum (Figure S12, Supporting Information) to that previously reported for **10**.[11]

■ ASSOCIATED CONTENT

Ⓢ Supporting Information

Spectroscopic data for complexes **2**−**9**, crystallographic details and data in CIF format, and computational details. This material is available free of charge via the Internet at http://pubs.acs.org.

■ AUTHOR INFORMATION

Corresponding Author

*E-mail: thomasc@brandeis.edu.

Notes

The authors declare no competing financial interest.

■ ACKNOWLEDGMENTS

We acknowledge the financial support of the U.S. Department of Energy under Award No. DE-SC0004019. C.M.T. is grateful for a 2011 Sloan Research Fellowship.

■ REFERENCES

(1) Lewis, N. S.; Nocera, D. G. *Proc. Nat. Acad. Sci. U.S.A.* **2006**, *103*, 15729−15735.
(2) Fachinetti, G.; Floriani, C.; Zanazzi, P. F. *J. Am. Chem. Soc.* **1978**, *100*, 7405−7407.
(3) Gambarotta, S.; Arena, F.; Floriani, C.; Zanazzi, P. F. *J. Am. Chem. Soc.* **1982**, *104*, 5082−5092.
(4) Yin, X.; Moss, J. R. *Coord. Chem. Rev.* **1999**, *181*, 27−59.
(5) Gade, L. H. *Angew. Chem., Int. Ed.* **2000**, *39*, 2658−2678.
(6) Wheatley, N.; Kalck, P. *Chem. Rev.* **1999**, *99*, 3379−3420.
(7) Cooper, B. G.; Napoline, J. W.; Thomas, C. M. *Catal. Rev. Sci. Eng.* **2012**, *54*, 1−40.
(8) Krogman, J. P.; Foxman, B. M.; Thomas, C. M. *J. Am. Chem. Soc.* **2011**, *133*, 14582−14585.
(9) Thomas, C. M. *Comments Inorg. Chem.* **2011**, *32*, 14−38.
(10) Greenwood, B. P.; Forman, S. I.; Rowe, G. T.; Chen, C.-H.; Foxman, B. M.; Thomas, C. M. *Inorg. Chem.* **2009**, *48*, 6251−6260.
(11) Greenwood, B. P.; Rowe, G. T.; Chen, C.-H.; Foxman, B. M.; Thomas, C. M. *J. Am. Chem. Soc.* **2010**, *132*, 44−45.
(12) Hoskin, A. J.; Stephan, D. W. *Organometallics* **1999**, *18*, 2479−2483.
(13) Jacoby, D.; Isoz, S.; Floriani, C.; Chiesi-Villa, A.; Rizzoli, C. *J. Am. Chem. Soc.* **1995**, *117*, 2805−2816.
(14) Jacoby, D.; Floriani, C.; Chiesi-Villa, A.; Rizzoli, C. *J. Am. Chem. Soc.* **1993**, *115*, 7025−7026.
(15) Mendiratta, A.; Figueroa, J. S.; Cummins, C. C. *Chem. Commun.* **2005**, 3403−3405.
(16) Silvia, J. S.; Cummins, C. C. *Chem. Sci.* **2011**, *2*, 1474−1479.
(17) Napoline, J. W.; Bezpalko, M. W.; Foxman, B. M.; Thomas, C. M. *Chem. Commun.* **2013**, DOI: 10.1039/C2CC35594A.
(18) Napoline, J. W.; Krogman, J. P.; Shi, R.; Kuppuswamy, S.; Bezpalko, M. W.; Foxman, B. M.; Thomas, C. M. Submitted for publication, 2013.
(19) Zhou, W.; Marquard, S. L.; Bezpalko, M. W.; Foxman, B. M.; Thomas, C. M. *Organometallics* **2013**, DOI: 10.1021/om301194g.
(20) Howard, W. A.; Parkin, G. *J. Am. Chem. Soc.* **1994**, *116*, 606−615.
(21) Howard, W. A.; Trnka, T. M.; Waters, M.; Parkin, G. *J. Organomet. Chem.* **1997**, *528*, 95−121.
(22) Roesky, H. W.; Singh, S.; Yusuff, K. K. M.; Maguire, J. A.; Hosmane, N. S. *Chem. Rev.* **2006**, *106*, 3813−3843.
(23) Setty, V. N.; Zhou, W.; Foxman, B. M.; Thomas, C. M. *Inorg. Chem.* **2011**, *50*, 4647−4655.
(24) Howard, W. A.; Waters, M.; Parkin, G. *J. Am. Chem. Soc.* **1993**, *115*, 4917−4918.
(25) Jany, G.; Fawzi, R.; Steimann, M.; Rieger, B. *Organometallics* **1997**, *16*, 544−550.
(26) Hillhouse, G. L.; Bercaw, J. E. *J. Am. Chem. Soc.* **1984**, *106*, 5472−5478.
(27) Kessler, M.; Hansen, S.; Hollmann, D.; Klahn, M.; Beweries, T.; Spannenberg, A.; Brückner, A.; Rosenthal, U. *Eur. J. Inorg. Chem.* **2011**, *2011*, 627−631.

(28) Cuerva, J. M.; Campaña, A. G.; Justicia, J.; Rosales, A.; Oller-López, J. L.; Robles, R.; Cárdenas, D. J.; Buñuel, E.; Oltra, J. E. *Angew. Chem., Int. Ed.* **2006**, *45*, 5522−5526.
(29) Frisch, M. J.; Trucks, G. W.; Schlegel, H. B.; Scuseria, G. E.; Robb, M. A.; Cheeseman, J. R.; Scalmani, G.; Braone, V.; Mennucci, B.; Petersson, G. A.; et al. *Gaussian 09*, Revision A.1; Gaussian, Inc.: Wallingford, CT, 2009. See Supporting Information for full reference.
(30) Glendening, E. D.; Reed, A. E.; Carpenter, J. E. *NBO*, Version 3.1.
(31) Jayarathne, U.; Chandrasekaran, P.; Jacobsen, H.; Mague, J. T.; Donahue, J. P. *Dalton Trans.* **2010**, *39*, 9662−9671.
(32) Sur, S. K. *J. Magn. Reson.* **1989**, *82*, 169−173.
(33) Evans, D. F. *J. Chem. Soc.* **1959**, 2003−2005.
(34) *Apex2*, Version 2 User Manual, M86-E01078; Bruker Analytical X-ray Systems: Madison, WI, 2006.
(35) Becke, A. D. *Phys. Rev. A* **1988**, *38*, 3098−3100.
(36) Perdew, J. P. *Phys. Rev. B* **1986**, *33*, 8822−8824.
(37) Hay, P. J.; Wadt, W. R. *J. Chem. Phys.* **1985**, *82*, 299−310.
(38) Dunning, T. H., Hay, P. J. In *Modern Theoretical Chemistry*; Schaefer, H. F., Ed.; Plenum: New York, 1976; pp 1−28.